Journal of ELECTRONIC MATERIALS, Vol. 50, No. 4, 2021
https://doi.org/10.1007/s11664-020-08480-5

ASIAN CONSORTIUM ACCMS–INTERNATIONAL CONFERENCE ICMG 2020

First Principle Study of Adsorption Behavior of PF_5 Gas Molecule on S and Mo Vacancy MoS_2 Monolayer

J. MERIBAH JASMINE,[1] C. PREFERENCIAL KALA,[1,2] and D. JOHN THIRUVADIGAL[1]

1.—Department of Physics and Nanotechnology, Centre for Materials Science and Nanodevices, SRM Institute of Science and Technology, Kattankulathur, Tamil Nadu 603203, India. 2.—e-mail: preferec@srmist.edu.in

The molybdenum disulfide monolayer (MoS_2) is gaining more attention due to its attractive electronic property, and it is extensively used in different electronic applications. The presence of vacancies on the MoS_2 monolayer leads to an increase in the conductivity of the material. In this work, we have investigated the adsorption behavior and estimated the gas-sensing properties of the S-vacancy (V_S) and the Mo-vacancy (V_{Mo}) MoS_2 monolayers and the two-probe MoS_2 devices with phosphorus pentafluoride (PF_5) gas molecule. To explore the sensing and electronic properties of V_S and V_{Mo} MoS_2 towards PF_5 gas adsorption, the adsorption distance, adsorption energy, charge transfer, band structure, and density of the states have been analyzed using density functional theory in combination with Non-Equilibrium Green's Function. The results show that the PF_5 gas molecule is allowed to adsorb on the S- and Mo-vacancy MoS_2 monolayers through van der Waals interaction. The PF_5 gas molecule shows adsorption distances of 3.3274 Å and 2.8673 Å, adsorption energies of − 0.1640 eV and − 0.3489 eV, and charge transfers of − 0.025 Q (e) and − 0.053 Q (e) on the V_S/V_{Mo} MoS_2 monolayers. To study the electron transport properties, the device density of the states, the transmission spectra, and the current–voltage characteristics of the V_S/V_{Mo} MoS_2 two-probe devices have been analyzed. The results predicted that the Mo-vacancy MoS_2 device shows relatively more adsorption towards the PF_5 gas molecule when compared with the V_S MoS_2 device.

Key words: Density functional theory (DFT), non-equilibrium Green's function (NEGF), phosphorus pentafluoride (PF_5), molybdenum disulfide (MoS_2), electron transport study, van der Waals interaction

INTRODUCTION

Two-dimensional (2D) materials like graphene and the materials from transition metal dichalcogenides (TMDs) have attracted interest due to their fascinating properties under ultra-thin thicknesses and the related quantum effects.[1–3] In the case of graphene, the presence of a zero bandgap has limited its process in many applications.[4–7] 2D TMD is a material which consists of one transition metal (M) and two chalcogenides (X_2) in the form of MX_2, which has extremely interesting prospects for next-generation optoelectronic and nano-electronic devices.[4,8,9] Among the TMDs, molybdenum disulfide monolayer (MoS_2) is considered to be a most promising new class of material. It has been successfully synthesized, and some of its unique distinguished characters can be used in numerous

(Received May 11, 2020; accepted September 9, 2020; published online October 10, 2020)

applications, such as gas sensors, transistors, photodetectors, energy storage devices, diodes, supercapacitors, etc.[4,6,7,10–12] Some important intrinsic merits of MoS_2 include its high surface to volume ratio, high conductivity, and semiconducting properties, which have helped the material become a gas sensor.[8,13,14] The presence of vacancies on the MoS_2 monolayer influences the sensing nature of the material for selective molecular adsorption. Yue et al. have suggested that H_2, O_2, H_2O, NH_3, NO, NO_2, and CO gas molecule are able to be adsorbed on the MoS_2 monolayer with small charge transfers. These gas molecule show some significant changes in the band structure and density of states (DOS) after the adsorption of the gas molecule.[14] Abbas et al. have suggested that the P and S atoms have similar covalent radii, and thus can easily form chemical bonds with the Mo atoms. They also explored the adsorption behavior of O_2 and NO gas of the P- and N-doped MoS_2 monolayers, and suggested that NO adsorption on the P-doped MoS_2 monolayer shows more adsorption than on the N-doped MoS_2 monolayer.[15] Ren et al. predicted that different defects show different effects of CH_3 adsorption on MoS_2 monolayers. They observed that CH_3 adsorption on S defects is more effective when compared with Mo defects.[16] Ramanathan reported that the doping or defect substitution on MoS_2 monolayers changes the electronic and chemical properties of the material and helps in boosting its sensing applications. They also concluded that MoS_2 can be a promising material for gas sensor applications in industry, due to its desirable direct bandgap and high surface to volume ratio.[5] Burman et al. proved experimentally that the presence of vacancy sites and contact electrodes show significant effects on the sensing characteristics.[17]

Environmental pollution by toxic pollutants is causing great concern worldwide. PF_5 is a colorless, toxic, non-flammable, compressed gas which causes irritation in the eyes, skin, and mucus membranes of human beings. When the gas is exposed to water, it will generate toxic corrosive fumes.[18–20] Therefore, the detection of toxic gases is extremely important for both public health and industry.[17] In this work, we systematically investigated the interaction of PF_5 gas molecule on V_S and V_{Mo} MoS_2 monolayers and MoS_2 devices using density functional theory (DFT) and the non-equilibrium Green's function (NEGF) to exploit the possibilities of MoS_2 being a PF_5 gas sensor. For a deeper understanding of the adsorption behavior, and to study the changes in the electronic properties, the adsorption energy, adsorption distance, band structure, DOS, charge transfer, transmission spectra, and I–V characteristics have been analyzed.

COMPUTATIONAL DETAILS

To explore the feasibility of V_S/V_{Mo} MoS_2 monolayers being considered as a PF_5 gas sensor, a model MoS_2 monolayer with S/Mo vacancies has been constructed in the presence and the absence of PF_5 gas molecule, as shown in Fig. 1. All the calculations have been performed using the Atomistix Toolkit [9,13,21] package based on DFT combined with NEGF.[22,23] Initially, we optimized the MoS_2 monolayer and the device with the S and Mo vacancies. Further, we optimized the structure in the presence and absence of PF_5 gas molecule. For both the MoS_2 monolayer and the MoS_2 device, we have used Double Zeta plus polarization for the linear combination of the atomic orbital basic set. To describe the exchange and correlation potential, the generalized gradient approximation (GGA) of the Perdew–Burke–Ernzerhof (PBE) functional has been used.[9,13] To correct the effect of the van der Waals interaction, the empirical correction scheme (DFT+D2) has been used.[24] For energy tolerance, we have fixed the convergence criteria to be 1.0×10^{-5} Ha. We have set 0.005 Å and 0.002 Ha/Å for the displacements of the geometrical optimization and the maximum force, respectively. For the accuracy calculation of total energy, the global cut-off has been fixed at 5.0 Å for the calculation of integrals in the real space grid. For geometric optimization, the k-point sample of the Monkhorst–Pack grid was set to $3 \times 3 \times 1$ along the x, y and z directions of the Brillouin zone.[9,25] In addition, we have constructed a $4 \times 4 \times 1$ super cell for the MoS_2 monolayer. The size of the bulk model has been chosen in such a way as to prevent the interaction between the MoS_2 monolayer and the PF_5 gas molecule. The self-consistent loop energy has been set to 10^{-6} Ha for static electronic structural calculations.[9,25] The hexagonal lattice parameter relaxation calculations were carried out using $a = b$=12.66 Å and c = 20.00 Å parameters. Using the conjugate gradient method, all the atoms are fully relaxed until the maximum absolute atomic forces become less than 0.05 eV/A.[9] For geometrical optimization, we have brought out the S- and Mo-vacancies on the top of the surface of the MoS_2 monolayer, as shown in Fig. 1. The electron transport properties have been analyzed using DFT combined with NEGF. We built a model structure of a MoS_2 device with S and Mo vacancies. (This is shown in Fig. 5, below.) The device consists of 50 and 100 Mo and S atoms, respectively. The MoS_2 device has been divided into three regions, namely the left electrode, a central scattering region, and the right electrode. The size of the central region has been fixed at 19.55 Å, which is long enough to study the adsorption behavior of the PF_5 gas molecule. The size of the left and right electrodes has been set at 3.16 Å in order to analyze the effect of adsorption between the V_S/V_{Mo} MoS_2 monolayer

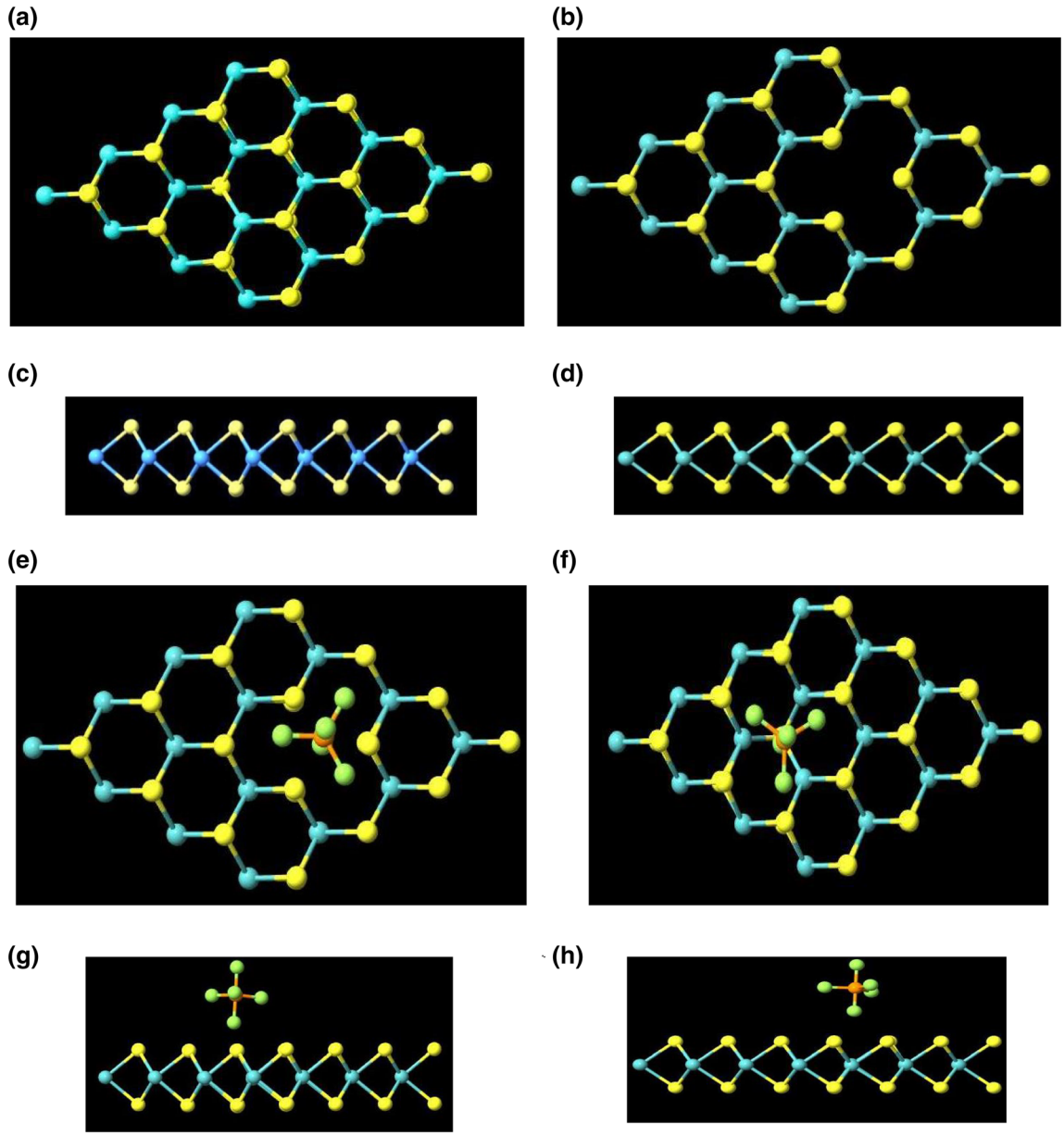

Fig. 1. (a–d) Optimized structure of top and side views of the V_S/V_{Mo} MoS_2 monolayer, (e–h) optimized structure of top and side views of PF_5 adsorption on the V_S/V_{Mo} MoS_2 monolayer.

and the PF_5 gas molecule. For geometric optimization, the k-point sample has been set at $2 \times 1 \times 100$ along the x, y and z directions of the Brillouin zone of the device. NEGF has been used to study the transmission coefficient of the incident electron, with energy, E, through the central region along the z direction.[22] The transmission function, $T(E, V)$, of the MoS_2 device at energy, E, has been calculated using NEGF formalism as:

$$T(E,V) = Tr\left[\Gamma_L(E,V)G^R(E)\Gamma_R(E,V)G^A(E)\right] \quad (1)$$

where Γ_L and Γ_R indicate the contact broadening functions of the left and right electrodes, respectively, and G^R and G^A the related Green's functions.

From the transmission function, $T(E, V)$, the current, $I(V)$, has been calculated using the Landauer formula:[22,26]

$$I(V) = \frac{2e^2}{h}\int_{\mu_L}^{\mu_R}\left[f(E-\mu_L) - f(E-\mu_R)\right]T(E,V)\mathrm{d}E \quad (2)$$

where e denotes the charge of the electron, h the Planks constant, $f(E - \mu_{L/R})$ the Fermi distribution of electrons along the left and right electrodes, E the energy of the electron, and μ_L and μ_R the electrochemical potential of the left and right electrodes, respectively.[26]

To quantitatively analyze the adsorption behavior and strength of the interaction of the PF_5 gas on the V_S/V_{Mo} MoS_2 monolayer, the adsorption energy has been calculated, and is given as:

$$E_{ads} = E_{PF_5\,V_{S/Mo}MoS_2} - \left(E_{V_{S/Mo}MoS_2} + E_{PF_5}\right) \quad (3)$$

where $E_{PF_5\,V_{S/Mo}MoS_2}$ denotes the total energy of the PF_5-adsorbed V_S/V_{Mo} MoS_2 monolayer, $E_{V_{S/Mo}MoS_2}$ denotes the energy of the V_S/V_{Mo} MoS_2 monolayer, and E_{PF_5} represents the total energy of the gas molecule.[9]

For the best adsorption orientation, we placed the PF_5 gas molecule on top of the vacancy created on the MoS_2 monolayer. The charge transfer calculation has been carried by the Mulliken population analysis in which the charge of the atom can be acquired by taking the difference between the value of the actual valance charge of each atom of the V_S/V_{Mo} MoS_2 monolayer and the charge acquired from the Mulliken population analysis. The total summation of all the difference values gives the net charge of the system. The charge transfer with a negative sign denotes that the charge is transferred from the system to the gas molecule, while a positive sign denotes that the charge is transferred from the gas molecule to the system.[9,27,28] The re-arrangement of charges after the adsorption of the PF_5 gas molecule plays an important role in obtaining better sensing and electronic properties.

To analyze the stability of the system, the structure formation energy has been estimated for the V_S/V_{Mo} MoS_2. The structural formation energy for the bulk system is defined as:

$$E_f = E_{V_{S/V_{Mo}}-MoS_2} - E_{MoS_2} + \mu_I \quad (4)$$

$E_{V_{S/V_{Mo}}}$ denotes the total energy of the system. E_{MoS_2} denotes the total energy of MoS_2 before vacancy creation, and μ_I denotes the chemical potential of the V_S/V_{Mo} MoS_2 monolayer.[9]

RESULTS AND DISCUSSION

The optimized structures of the V_S/V_{Mo} MoS_2 monolayer in the presence and absence of PF_5 gas molecule is shown in Fig. 1. The estimated formation energies of the V_S and V_{Mo} MoS_2 monolayers are 2.549 eV and 7.927 eV, respectively.[9,29–33] After the adsorption, the structure of the PF_5 gas molecule experience a small change, where the bond length between P and F has been reduced from 158 pm to 157 pm for the V_S and 157.5 pm for the V_{Mo} MoS_2. The bond angle, F–P–F, is decreased from 120° and 90° to 119.70° and 89.6° for the V_S and 118.21° and 88.8° for the V_{Mo} MoS_2. To obtain a deeper understanding of the V_S/V_{Mo} MoS_2 monolayer towards the PF_5 gas molecule, the adsorption distance, adsorption energy, and charge transfer of V_S and V_{Mo} have been calculated and are shown in Table I. The shortest distance between the atoms of the PF_5 gas molecule and the atoms of the V_S/V_{Mo} MoS_2 is defined as the adsorption distance. For PF_5 adsorption, we obtained the adsorption distances of 3.3274 Å and 2.8673 Å for the V_S and V_{Mo} MoS_2, respectively. To quantitatively analyze the adsorption behavior of MoS_2 towards the PF_5 gas molecule, the adsorption energy has been calculated. The calculated adsorption energy values are − 0.1640 eV and − 0.3489 eV for the V_S and V_{Mo} MoS_2 monolayer. To analyze the strength of the interaction between the V_S/V_{Mo} MoS_2 monolayer and the PF_5 gas molecule, the charge transfer has been calculated. Due to the charge transfer, there is a change in the conductivity of the MoS_2 monolayer. The change in the conductivity acts as an important key factor to determine the sensing behavior of the system.[34] We obtained a charge transfer of − 0.025 Q (e) for the V_S and − 0.053 Q (e) for the V_{Mo} MoS_2 monolayers. Here, the negative sign denotes that the charge transfer is taking place from the V_S/V_{Mo} MoS_2 to PF_5 gas molecule. All the structural analysis shows that the V_{Mo} MoS_2 shows more adsorption towards PF_5 when compared with the V_S MoS_2 monolayer. There is no bond formation between the V_S/V_{Mo} MoS_2 and the PF_5 gas molecule, which denotes that the adsorption was caused due to a weaker interactive force called the van der Waals interaction. Figure 2 represents the comparison results of the adsorption energy, charge transfer, and adsorption distance of V_S MoS_2 and V_{Mo} MoS_2. From Fig. 2a and b, we can see that the adsorption energy and charge transfer of V_{Mo} MoS_2 is more when compared with V_S MoS_2. From Fig. 2c, we can see that the adsorption distance of V_{Mo} MoS_2 is smaller than the V_S MoS_2 device. The smaller the adsorption distance, stronger the interaction between the MoS_2 monolayer and the PF_5 gas molecule,[35] which shows that PF_5 adsorption on V_{Mo} MoS_2 has a greater interaction than on V_S MoS_2.

Table I. Values of adsorption distance, band gap, adsorption energy, and charge transfer of the MoS_2 monolayer and the MoS_2 device

MoS_2 model	V_S/V_{Mo} vacancies	Adsorption distance d (Å)	Adsorption energy E_{ads} (eV)	Charge transfer Q (e)
MoS_2 monolayer	V_S	3.3274	− 0.1640	− 0.025
	V_{Mo}	2.8673	− 0.3489	− 0.053

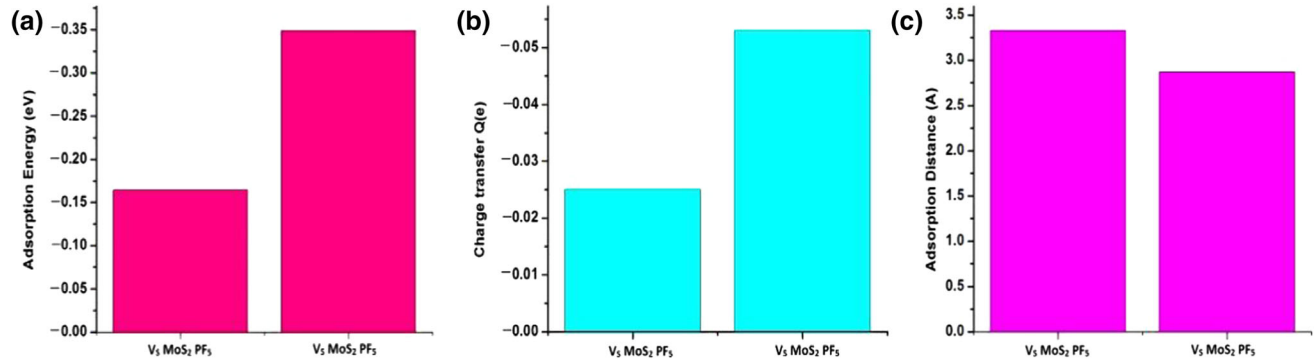

Fig. 2. (a) Calculated adsorption energy, (b) charge transfer, and (c) adsorption distance of V_S/V_{Mo} MoS_2 PF_5.

Figure 3 represents the band structure of the V_S/V_{Mo} MoS_2 monolayer before and after adsorption of the PF_5 gas molecule along the high symmetry k points of (Γ–M–K–Γ) of the Brillouin zone.[28,36–39] $V_S MoS_2$ shows an indirect band gap of 1.033 eV and V_{Mo} MoS_2 shows a direct band gap of 0.223 eV. After the adsorption of the PF_5 gas molecule, we observed that the band gap has increased to 1.235 eV for V_S MoS_2 and PF_5 and to 0.430 eV for V_{Mo} MoS_2 PF_5. The adsorption of PF_5 also causes some significant changes in the band structure. This implies that the adsorption of the PF_5 gas molecule affects the electrical conductivity of the V_S/V_{Mo} MoS_2 monolayer.

To analyze the electronic properties of the PF_5 gas adsorption on the V_S/V_{Mo} MoS_2, the total electronic density of states (TDOS) has been studied before and after the adsorption of the gas molecule.[40] The TDOS of V_S MoS_2 (Fig. 4a) shows some small changes near the Fermi level where the band gap of V_S MoS_2 is slightly increased after the adsorption of the gas molecule. This will subsequently affect the electronic property of the material after the adsorption. For the creation of the Mo vacancy, a peak appears exactly at the Fermi level, which also indicates an increase in the electrical conductivity of V_{Mo} MoS_2. In Fig. 4f, the projected density of state (PDOS) shows that the increase in the peak is caused due to the p and d orbitals of the V_{Mo} MoS_2 monolayer. The TDOS for PF_5 adsorption on the V_{Mo} MoS_2 shows a significant change near the Fermi level where the peak of TDOS at the Fermi level has been slightly reduced after the adsorption of the gas molecule, which indicates that there will be a reduction in the current after the adsorption of the molecule. Moreover, we observed that the adsorption causes some changes in the peaks of TDOS between − 5 eV and 5 eV after the adsorption on the V_S/V_{Mo} MoS_2. These changes indicate that the TDOS of V_S MoS_2 is considerably affected by PF_5 gas adsorption. Figure 4c–f shows the PDOS of V_S/V_{Mo} MoS_2 with and without the PF_5 gas molecule. From the PDOS, we can see that the changes in the peaks are caused due to the overlapping of the p and d orbitals of PF_5 and the V_S/V_{Mo} MoS_2 monolayer.

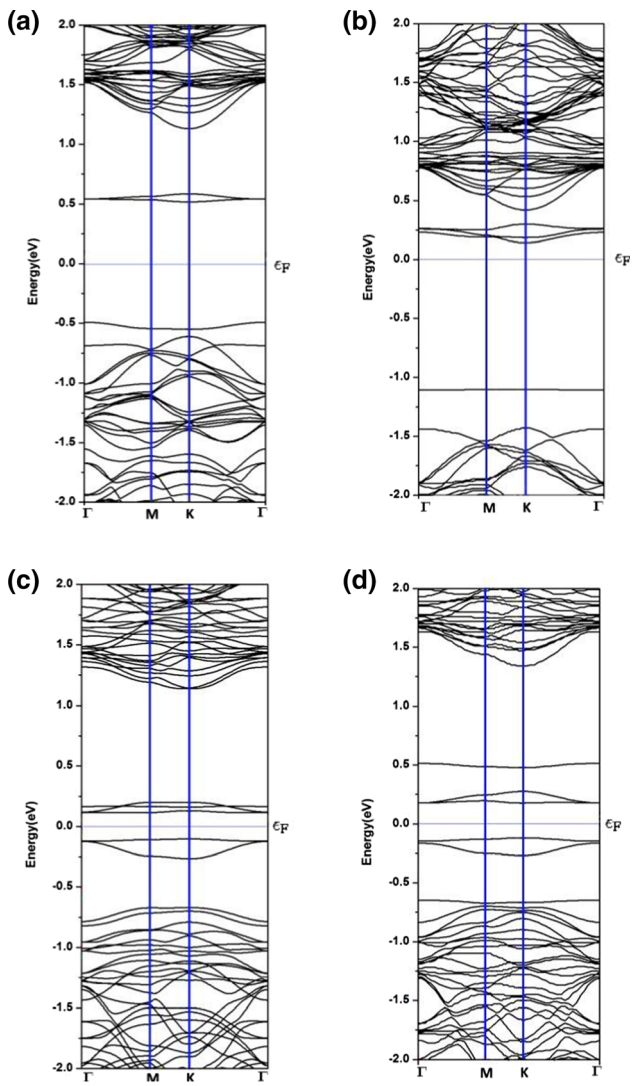

Fig. 3. (a, c) Band structure of the V_S/V_{Mo} MoS_2 monolayer, and (b, d) band structure of the V_S/V_{Mo} MoS_2 monolayer after adsorption of the PF_5 gas molecule.

Figure 5a and b shows the optimized device structure of the V_S/V_{Mo} two-probe MoS_2 device, while Fig. 5c and d shows the V_S and V_{Mo} MoS_2 devices after the adsorption of the PF_5 gas molecule,

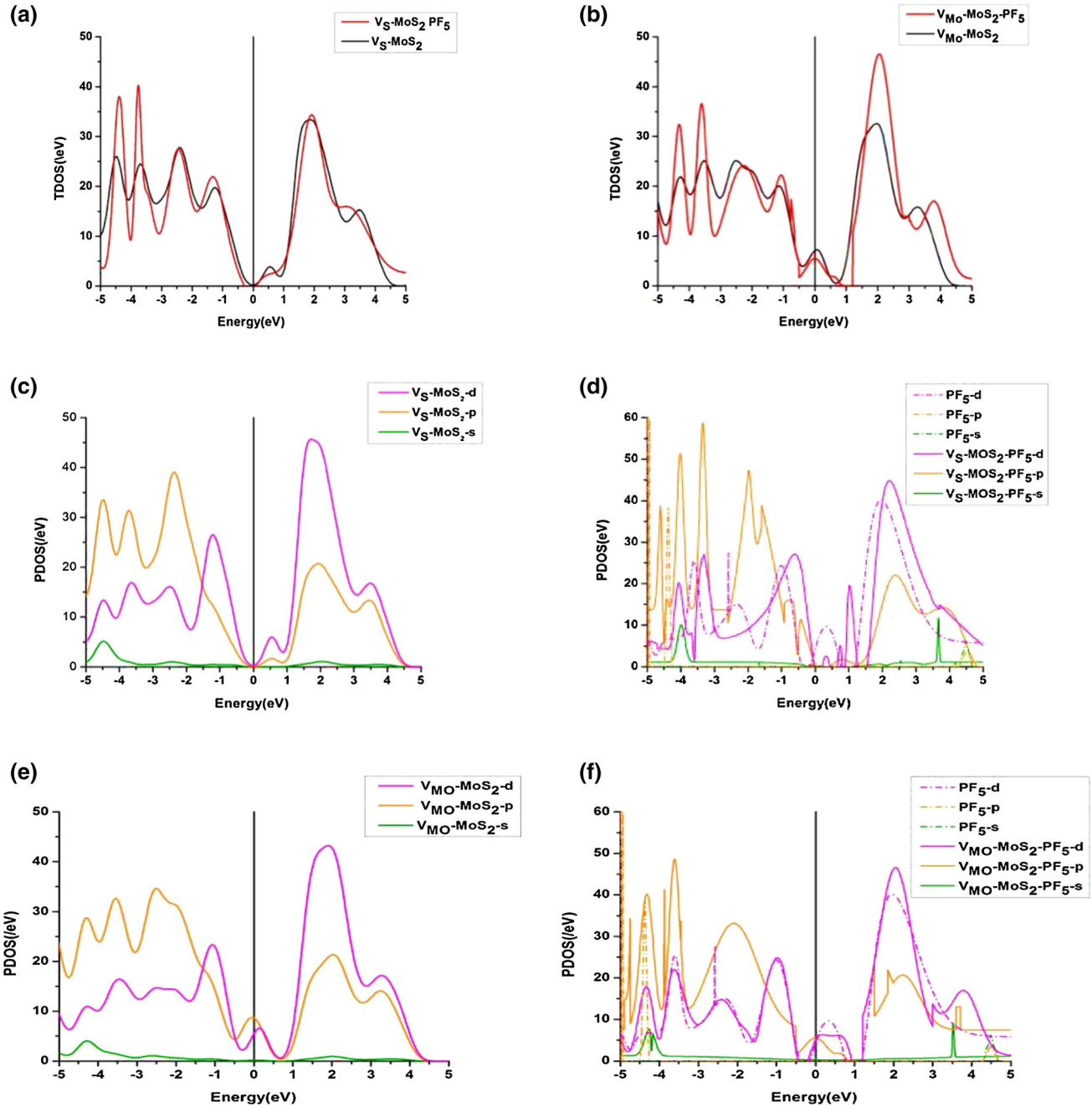

Fig. 4. (a, b) TDOS of the V_S MoS_2 and the V_{Mo} MoS_2, respectively, (c, d) PDOS of V_S MoS_2 and the V_S MoS_2 PF_5 device, respectively, and (e, f) PDOS of V_{Mo} MoS_2 and the V_{Mo} MoS_2 PF_5 device, respectively.

demonstrating that there is no bond formation between the V_S/V_{Mo} MoS_2 device and the PF_5 gas molecule. The device density of states (DDOS) and the transmission spectra calculations, which were performed for the V_S/V_{Mo} MoS_2 device by applying bias voltage to the electrodes in the presence and absence of the PF_5 gas molecule, are shown in Fig. 6a and b. The Fermi energy, E_F, is set to zero eV for all the curves. From Figs. 4b and 6a, we can see that the adsorption of PF_5 does not cause any changes in the band gap, but that all the DDOS peaks between − 0.8 eV and 0.8 eV in both cases have been decreased after the adsorption of PF_5. The peaks in the DDOS confirm the peaks in the transmission spectra. Figure 7c and d shows the transmission spectra of the V_S/V_{Mo} MoS_2 device. From Fig. 7, we can see that there is a wide transmission gap near the Fermi level which indicates that the transmission co-efficient is zero in this region, which acts as a barrier for electron transmission. Moreover, there is a significant decrease in the electron transmission coefficient

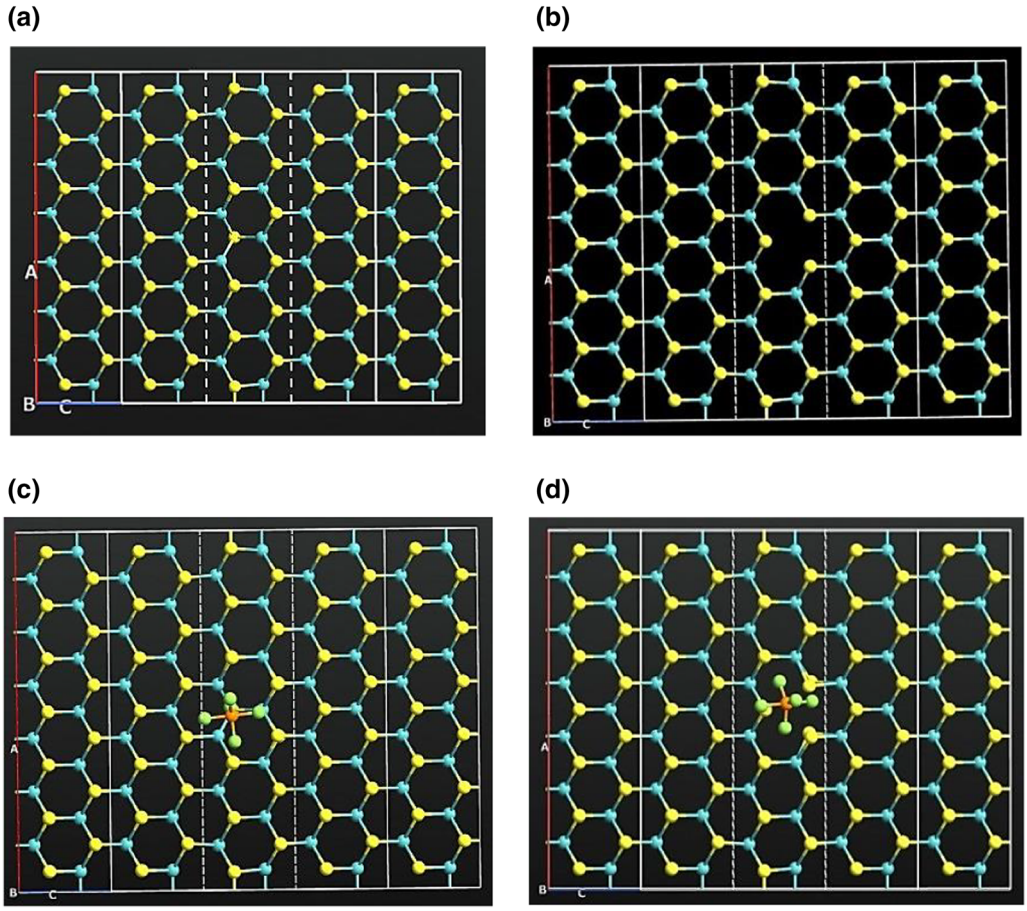

Fig. 5. (a, b) Optimized structure of the V_S/V_{Mo} MoS_2 device, and (c, d) optimized structure of PF_5 adsorption on the V_S/V_{Mo} MoS_2 device.

after the adsorption of the PF_5 gas molecule. The transmission peaks indicate that the conducting channels and the reduction of the transmission peaks may lead to a reduction in the current.[41] The decrease in the peaks of DDOS and the transmission spectra indicate that the V_S/V_{Mo} MoS_2 device is considerably affected by the PF_5 gas molecule.

CURRENT–VOLTAGE (*I–V*) CHARACTERISTICS

The *I–V* characteristics have been calculated and plotted to observe the changes in the conductivity and to analyze the performance of the V_S/V_{Mo} MoS_2 device as a PF_5 gas sensor. Figure 7 shows the *I–V* characteristics of the V_S/V_{Mo} MoS_2 device with and without the PF_5 gas molecule. From Fig. 7a, we can see that the current value for the V_S MoS_2 monolayer is zero until the applied voltage is 0.6 V. This can be caused due to the presence of a transmission gap in the transmission spectrum (Fig. 6c), which acts as a barrier. By increasing the applied voltage beyond 0.6 V, the current starts to increase linearly. For the V_S MoS_2 PF_5, the increase in the current is slightly less when compared with the V_S MoS_2, which is due to the reduction in the transmission peaks of the V_S MoS_2 device after adsorption of the PF_5 gas molecule. From Fig. 7b, it can be clearly seen that the flow of current is zero up to 0.6 V for the V_{Mo} MoS_2 device and zero up to 0.8 V after the adsorption of the PF_5 gas molecule. The reduction in the current can be caused due to the reduction in the transmission peaks (Fig. 6) after the adsorption. The changes in the current indicate that the V_S/V_{Mo} MoS_2 device is considerably affected by PF_5 adsorption.

To further understand the affinity of the PF_5 gas molecule towards the V_S/V_{Mo} MoS_2 device, the sensitivity of the material has been calculated, and is defined as:[22,42]

$$S = |G - G_0|/G_0 \quad (5)$$

where G and G_0 represent the conductance of the V_S/V_{Mo} MoS_2 monolayer before and after adsorption of the gas molecule.[22,42–44] The obtained results are shown in Table II, and reveal that the sensitivity of PF_5 adsorption on the V_{Mo} MoS_2 is comparatively more than the V_S MoS_2 for all bias voltages. For a bias voltage of 1.0 V, the sensitivity is 78.98% for V_S MoS_2 and 90.08% for V_{Mo} MoS_2. This shows that the PF_5 adsorption on V_{Mo} MoS_2 is comparatively more than on V_S MoS_2.

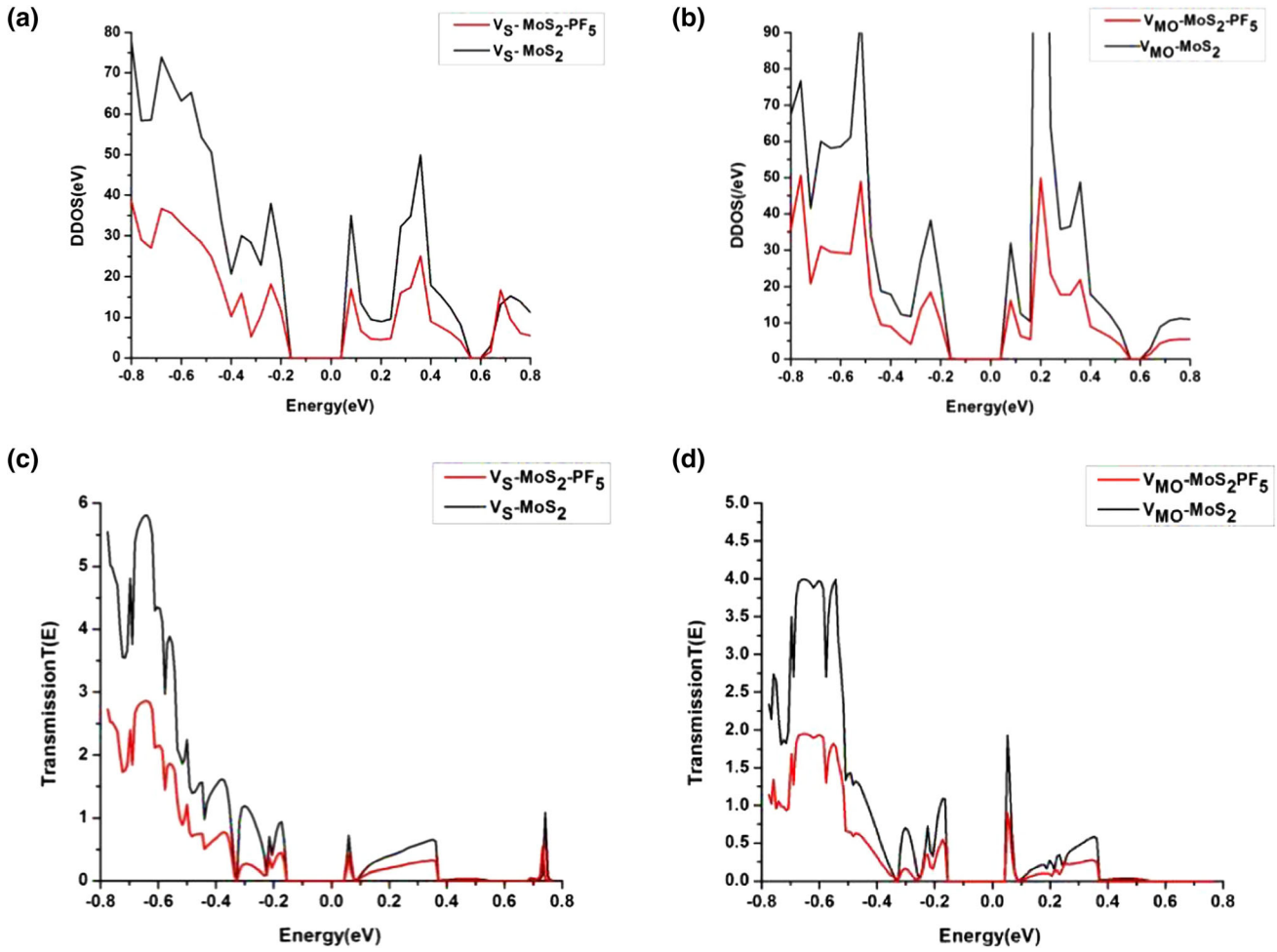

Fig. 6. (a, b) DDOS of the V_S and V_{Mo} MoS_2, respectively, and (c, d) transmission spectra of the V_S/V_{Mo} MoS_2 before and after adsorption of the PF_5 gas molecule.

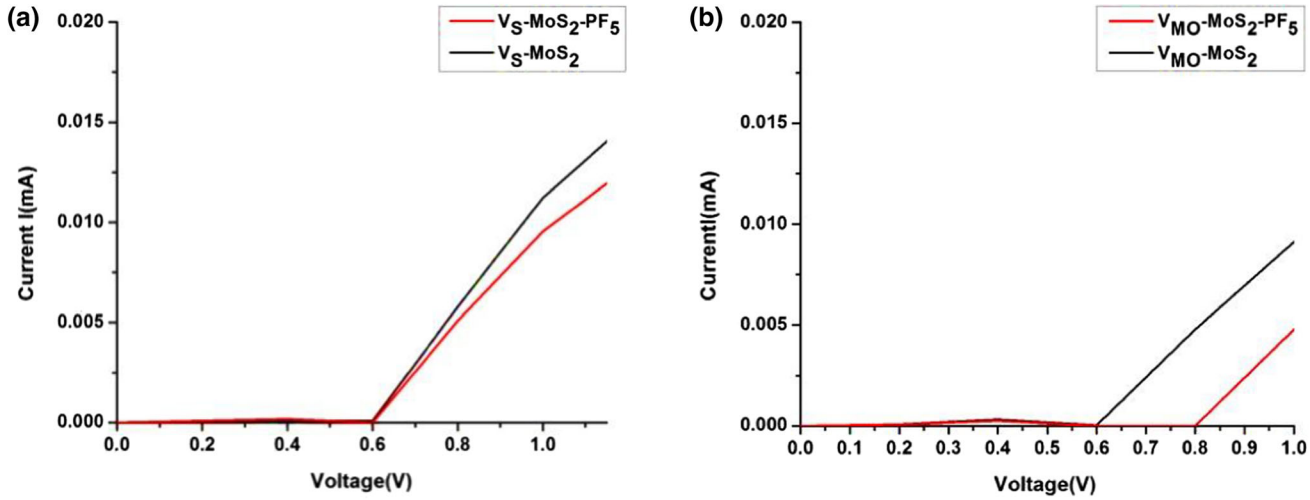

Fig. 7. (a, b) *I–V* characteristics of the V_S and V_{Mo} MoS_2, respectively.

Table II. Values of percentage of sensitivity under bias voltage from 0 to 1.0 V

	Percentage of sensitivity for the V_S/V_{Mo} MoS_2 device model	
Bias voltage (V)	**V_S MoS_2**	**V_{Mo} MoS_2**
0	10.65	11.58
0.2	12.23	15.85
0.4	36.34	45.35
0.6	15.25	23.46
0.8	48.52	69.67
1.0	78.98	90.08

CONCLUSION

We have explored the adsorption behavior and electron transport property of a V_S/V_{Mo} MoS_2 monolayer using DFT and NEGF. The structural stability of the V_S/V_{Mo} MoS_2 has been studied with the help of formation energy. To understand the adsorption properties of the V_S/V_{Mo} MoS_2 towards PF_5 gas molecule, the adsorption distance, adsorption energy, and charge transfer have been studied. The results show that the gas molecule are able to be adsorbed on the V_S/V_{Mo} MoS_2 monolayer by van der Waals interaction. The electron transport behavior of the V_S/V_{Mo} MoS_2 device were studied and the results are discussed. From the transmission spectra analysis, we found that the adsorption of the PF_5 gas shows a remarkable decrease in the transmission for the V_S/V_{Mo} MoS_2 device after the PF_5 adsorption. Thus, there is a significant reduction in the *I–V* curve for both the V_S and V_{Mo} MoS_2 devices. PF_5 adsorption on the V_{Mo} MoS_2 device shows more changes in the *I–V* curve when compared with PF_5 adsorption on the V_S MoS_2 device. Moreover, the evaluated sensitivity values show that the sensitivity is comparatively more in V_{Mo} MoS_2. All the analyses show that the PF_5 gas molecule strongly influence the V_{Mo} MoS_2 device when compared with the V_S MoS_2 device. Thus, we concluded that the V_{Mo} MoS_2 has an efficient role for sensing PF_5 gas molecule when compared with the V_S MoS_2.

ACKNOWLEDGMENTS

We gratefully acknowledge financial support for this project from DST-FIST, Government of India (Ref. No. SR/FST/PSI-155/2010). The authors convey their sincere thanks to Mrs. K. Janani Sivasankar, Assistant Professor, Department of Physics and Nanotechnology, SRMIST for their valuable support.

FUNDING

Department of Science and Technology, Ministry of Science and Technology (SR/FST/PSI-155/2010).

CONFLICT OF INTEREST

Authors declare that there is no conflict of interest.

REFERENCES

1. K.S. Novoselov, D. Jiang, F. Schedin, T.J. Booth, V.V. Khotkevich, S.V. Morozov, and A.K. Geim, *Proc. Natl. Acad. Sci. USA* 102, 10451 (2005).
2. C. Lee, R. Sundharam, M. Jaiswal, Y. Lu, and S. Hofmann, *J. Phys. D Appl. Phys.* 50, 440401 (2017).
3. Q. Wang, P. Wu, G. Cao, and M. Huang, *J. Phys. D Appl. Phys.* 46, 505308 (2013).
4. W. Ju, T. Li, X. Su, H. Li, X. Li, and D. Ma, *Phys. Chem. Chem. Phys.* 19, 20735 (2017).
5. A.A. Ramanathan and I.O.P. Conf, *Ser. Mater. Sci. Eng.* 305, 012001 (2018).
6. D. Voiry, J. Yang, and M. Chhowalla, *Adv. Mater.* 28, 6197 (2016).
7. D.J. Late, Y.K. Huang, B. Liu, J. Acharya, S.N. Shirodkar, J. Luo, A. Yan, D. Charles, U.V. Waghmare, V.P. Dravid, and C.N.R. Rao, *ACS Nano* 7, 4879 (2013).
8. B. Cho, M.G. Hahm, M. Choi, J. Yoon, A.R. Kim, Y.J. Lee, S.G. Park, J.D. Kwon, C.S. Kim, M. Song, Y. Jeong, K.S. Nam, S. Lee, T.J. Yoo, C.G. Kang, B.H. Lee, H.C. Ko, P.M. Ajayan, and D.H. Kim, *Sci. Rep.* 5, 8052 (2015).
9. J.M. Jasmine, A. Aadhityan, C.P. Kala, and D.J. Thiruvadigal, *Appl. Surf. Sci.* 489, 841 (2019).
10. N. Izyumskaya, D.O. Demchenko, V. Avrutin, Ü. Özgür, and H. Morkoç, *Turk. J. Phys.* 38, 478 (2014).
11. S.Y. Cho, S.J. Kim, Y. Lee, J.S. Kim, W. Bin Jung, H.W. Yoo, J. Kim, and H.T. Jung, *ACS Nano* 9, 9314 (2015).
12. H. Yang, Y. Liu, C. Gao, L. Meng, Y. Liu, X. Tang, and H. Ye, *J. Phys. Chem. C* 123, 30949 (2019).
13. B. Zhao, C. Shang, N. Qi, Z.Y. Chen, and Z.Q. Chen, *Appl. Surf. Sci.* 412, 385 (2017).
14. Q. Yue, Z. Shao, S. Chang, and J. Li, *Nanoscale Res. Lett.* 8, 1 (2013).
15. H.G. Abbas, T.T. Debela, S. Hussain, and I. Hussain, *RSC Adv.* 8, 38656 (2018).
16. J. Ren, H. Liu, Y. Xue, and L. Wang, *Nanoscale Res. Lett.* 14, 293 (2019).
17. D. Burman, R. Ghosh, S. Santra, S. Kumar Ray, and P. Kumar Guha, *Nanotechnology* 28 (2017).
18. V. Vincent and J. Forensic, *Leg. Investig. Sci.* 1, 005 (2015).
19. F. Larsson, P. Andersson, P. Blomqvist, A. Lorén, and B.E. Mellander, *J. Power Sources* 271, 414 (2014).
20. R. Chaurasiya and A. Dixit, *Phys. Chem. Chem. Phys.* 22, 13903 (2020).
21. H. Li, M. Huang, and G. Cao, *Phys. Chem. Chem. Phys.* 18, 15110 (2016).
22. A. Shokri and N. Salami, *Sensors Actuators B* 236, 378 (2016).
23. W. Jin, Y. Guofeng, X. Junjun, L. Jianming, C. Qing, C. Dunjun, L. Hai, Z. Rong, and Z. Youdou, *Sci. Rep.* 8, 6 (2018).
24. C.V. Nguyen, N.N. Hieu, and D.T. Nguyen, *Nanoscale Res. Lett.* 10, 1 (2015).
25. D. Chen, X. Zhang, J. Tang, H. Cui, and Y. Li, *Appl. Phys. A* 124, 194 (2018).
26. C.P. Kala and D.J. Thiruvadigal, *J. Comput. Electron.* 17, 580 (2018).
27. K. Janani and D. John Thiruvadigal, *Appl. Surf. Sci.* 418, 406 (2017).
28. W. Xu, P. Li, S. Li, B. Huang, C. Zhang, and P. Wang, *Physica E* 73, 83 (2015).
29. D. Cao, H.B. Shu, T.Q. Wu, Z.T. Jiang, Z.W. Jiao, M.Q. Cai, and W.Y. Hu, *Appl. Surf. Sci.* 361, 199 (2016).
30. J. Noh, H. Kim, and Y. Kim, *Phys. Rev. B* 89, 205417 (2014).
31. Y. Cheng, Z. Zhu, W. Mi, Z. Guo, and U. Schwingenschlogl, *Phys. Rev. B* 87, 100401(R) (2013).
32. W. Wang, C. Yang, L. Bai, M. Li, and W. Li, *Nanomaterials* 8, 74 (2018).

33. M.G. Sensoy, D. Vinichenko, W. Chen, C.M. Friend, and E. Kaxiras, *Phys. Rev. B* 95, 1 (2017).
34. S. Sivasathya, D.J. Thiruvadigal, and S.M. Jaya, *Chem. Phys. Lett.* 609, 76 (2014).
35. S. Zhao, J. Xue, and W. Kang, *Chem. Phys. Lett.* 595–596, 35 (2014).
36. M. Sharma, A. Kumar, P.K. Ahluwalia, A. Kumar, and P.K. Ahluwalia, *Physica E* 107, 117 (2019).
37. L. Feng, A. Li, J. Su, Y. Zhang, and Z. Liu, *Mater. Chem. Phys.* 209, 146 (2018).
38. C. Liu, H. Dong, Y. Ji, T. Hou, and Y. Li, *Sci. Rep.* 8, 1 (2018).
39. S. Ahmad and S. Mukherjee, *Graphene* 03, 52 (2014).
40. S.C. Lu and J.P. Leburton, *Nanoscale Res. Lett.* 9, 1 (2014).
41. W.H. Khoo and S.M. Sultan, in *IEEE Int. Conf. Semicond. Electron. Proceedings, ICSE*, pp. 221–224 (2014).
42. J. Pang, Q. Yang, X. Ma, L. Wang, C. Tan, D. Xiong, H. Ye, and X. Chen, *Phys. Chem. Chem. Phys.* 19, 30852 (2017).
43. X. Zhang, H. Cui, and Y. Gui, *Sensors* 17, 363 (2017).
44. X.P. Chen, L.M. Wang, X. Sun, R.S. Meng, J. Xiao, H.Y. Ye, and G.Q. Zhang, *IEEE Electron Device Lett.* 38, 661 (2017).